# SUPPORTING INFORMATION

# On the Structure of Ce-containing Silicophosphate Glasses: a Core-Shell Molecular Dynamics Investigation.

*Elisa Gambuzzi and Alfonso Pedone\**

Dipartimento di Scienze Chimiche e Geologiche, Università degli Studi di Modena e Reggio Emilia

via G. Campi, 183; 41125 Modena (Italy)

**Table S1.** Comparison between the experimental densities ($\rho_{exp}$)[1] and the ones computed with the PRIVEN method ($\rho_{PRIVEN}$) and after NPT MD simulations at 300K ($\rho_{NPT}$). The percentage difference between $\rho_{exp}$ and $\rho_{NPT}$ is also reported.

| Glass | $\rho_{exp}$ (g/cc) | $\rho_{PRIVEN}$ (g/cc) | $\rho_{NPT}$ (g/cc) | $[(\rho_{NPT}-\rho_{exp})/\rho_{xep}]\cdot100$ |
|---|---|---|---|---|
| CSP2 | 2.58 (±0.01) | 2.54 | 2.50 | - 3.10 % |
| CSP3 | 2.70 (±0.01) | 2.66 | 2.61 | - 3.33 % |
| CSP4 | 2.80 (±0.01) | 2.83 | 2.73 | - 2.50 % |
| CSP6 | 2.98 (±0.01) | 3.30 | 3.15 | + 5.70 % |
| CSP9 | 3.08 (±0.02) | 3.36 | 3.19 | + 3.57 % |

**Table S2**. Coordination number distributions of $Ce^{3+}$ and $Ce^{4+}$ calculated on 3 simulation boxes per composition (standard deviations in parenthesis).

| | 5 | 6 | 7 | 8 | 9 |
|---|---|---|---|---|---|
| | | | $Ce^{3+}$ | | |
| CSP2 | 5.3(0.8) | 37.0(13.3) | 45.9(11.4) | 11.7(4.4) | 0.1 (0.4) |
| CSP3 | 5.6(4.4) | 41.6(5.5) | 45.1(4.3) | 7.2(5.5) | 0.2(0.1) |
| CSP4 | 7.6(2.5) | 43.6(4.3) | 39.7(0.9) | 8.6(2.8) | 0.5(0.1) |
| CSP6 | 7.2(1.9) | 40.4(0.3) | 42.0 (1.3) | 9.5(1.7) | 0.9 (0.1) |
| CSP9 | 5.8(1.2) | 44.7(4.1) | 38.5 (3.4) | 9.6(2.8) | 1.4 (0.5) |
| | | | $Ce^{4+}$ | | |
| CSP6 | 0.0(0.0) | 0.0(0.0) | 66.7(11.3) | 33.3(4.1) | 0.0(0.0) |
| CSP9 | 0.0(0.0) | 0.0(0.0) | 34.4(10.6) | 65.5(10.5) | 0.1(0.1) |

**Table S3**. $Q^n$ species distributions of P and Si. Populations are given in percentage (pop. %) with respect to the total number of P or Si in the models.

| | $Q^0$ | $Q^1$ | $Q^2$ | $Q^3$ | $Q^4$ |
|---|---|---|---|---|---|
| | | | P | | |
| CSP2 | 0.0 | 0.7(0.1) | 33.2(2.5) | 60.2(3.1) | 4.9(0.4) |
| CSP3 | 0.4(0.1) | 2.3(0.3) | 45.2(1.3) | 49.1(0.2) | 2.3(0.5) |
| CSP4 | 0.7(0.1) | 4.9(0.5) | 53.8(0.3) | 38.8(1.5) | 1.1(0.9) |
| CSP6 | 1.9(0.4) | 14.2(1.2) | 67.9(2.5) | 15.2(0.5) | 0.0(0.0) |
| CSP9 | 2.2(0.3) | 16.7(1.4) | 69.0(3. 9) | 10.7(1.7) | 0.0(0.0) |
| | | | Si | | |
| CSP2 | 0.0(0.0) | 0.0(0.0) | 0.0(0.0) | 4.7(1.0) | 89.5(1.6) |
| CSP3 | 0.0(0.0) | 0.0(0.0) | 0.0(0.0) | 6.5(0.5) | 91.2(1.1) |
| CSP4 | 0.0(0.0) | 0.0(0.00) | 0.0(0.00) | 5.2(0.1) | 90.7(0.3) |
| CSP6 | 0.0(0.0) | 0.0(0.0) | 0.0(0.0) | 5.2(3.9) | 90.8(4.0) |

**Table S4**. Average number $n$ of BOs bonded to P atoms, $\bar{n}_{P(Qn)}$, $Ce_2O_3$ content, Si/P, Ce/P ratios and the average number of NBOs bonded to P and available for Ce coordination, $NBO^P/Ce$.

| Glasses | $\bar{n}_{P(Qn)}$ | $Ce_2O_3$ (mol%) | Si/P | Ce/P | $NBO^P/Ce$ |
|---|---|---|---|---|---|
| CSP2 | 2.7 | 2.2 | 0.867 | 0.06 | 16.61 |
| CSP3 | 2.5 | 4.1 | 0.711 | 0.11 | 11.08 |
| CSP4 | 2.3 | 7.5 | 0.508 | 0.17 | 8.29 |
| CSP6 | 2.0 | 18.2 | 0.140 | 0.29 | 6.10 |
| CSP9 | 1.9 | 28.3 | 0.004 | 0.33 | 6.15 |

**Table S5**. $R_P^{P/Si}$ and $R_{Si}^{P/Si}$ values as a function of the $n°Ce/(n°P+n°Si)$ ratio, which characterizes each composition.

| $n°Ce/(n°P+n°Si)$ | $R_P^{P/Si}$ | $R_{Si}^{P/Si}$ |
|---|---|---|
| 0.03 (CSP2) | 0.492 | 0.864 |
| 0.06 (CSP3) | 0.496 | 0.828 |
| 0.11 (CSP4) | 0.507 | 0.713 |
| 0.25 (CSP6) | 0.495 | 0.606 |

**Table S6**. Populations of $Q^n$ sites (4-coordinated former cations bonded to $n$ bridging oxygens), 5-coordinated ($P^5$) and 6-coordinated ($H^6$) former cations in the CSP models. Comparing Rigid ion and Core Shell output data of statistical analysis performed as mentioned in the *Method* section.

| | $Q^0$ | $Q^1$ | $Q^2$ | $Q^3$ | $Q^4$ | $P^5$ | $H^6$ |
|---|---|---|---|---|---|---|---|
| | | | | Si | | | |
| Rigid ion | 0.0 | 0.0 | 0.3 | 12.0 | 83.3 | 4.4 | 0.0 |
| Core-Shell | 0.0 | 0.0 | 0.0 | 6.9 | 89.2 | 3.9 | 0.0 |
| | | | | P | | | |
| Rigid ion | 0.3 | 2.9 | 29.9 | 49.8 | 16.5 | 0.5 | 0.0 |
| Core shell | 0.4 | 3.5 | 59.7 | 35.7 | 0.7 | 0.0 | 0.0 |

**Table S7**. Comparison of $Q^n$ site population of the CaO-$P_2O_5$ glass determined by NMR experiments, rigid ion and core-shell MD simulations.

| | $Q^0$ | $Q^1$ | $Q^2$ | $Q^3$ | $Q^4$ |
|---|---|---|---|---|---|
| Experimental[2] | 0 | 4 | 96 | 0 | 0 |
| Rigid ion | 1 | 23 | 51 | 21 | 5 |
| Core shell | 0 | 11 | 80 | 9 | 0 |

**Table S8**. Description of the second coordination shells of $Ce^{3+}$ and $Ce^{4+}$ by the Rigid ion[3] and the Core Shell (this work) models. Cutoff distances for coordination numbers are the same adopted by Du et al[3]: 4.37/4.00 Å for $Ce^{3+}/Ce^4$.

| | $Ce^{3+}$ | | $Ce^{4+}$ | |
|---|---|---|---|---|
| | **Si** | **P** | **Si** | **P** |
| Rigid Ion | 1.2 | 5.7 | 1.2 | 4.9 |
| Core shell | 0.4 | 6.4 | 1.0 | 6.8 |

**Table S9**. Analysis of $Ce^{3+}$ second coordination sphere within a 5.00 Å radius cutoff. Coordination numbers with respect to P, ($CN_{Ce}^P$), Si, ($CN_{Ce}^{Si}$), and Al, ($CN_{Ce}^{Al}$) versus the amount of $Ce_2O_3$ (mol %) in the composition.

| $Ce_2O_3$ mol % | $CN_{Ce}^P$ | $CN_{Ce}^{Si}$ | $CN_{Ce}^{Al}$ |
|---|---|---|---|
| | $Ce^{3+}$ | | |
| 2.2  (CSP2) | 7.99(0.26) | 1.30(0.12) | 0.08(0.05) |
| 4.1  (CSP3) | 7.91(0.15) | 1.56(0.07) | 0.12(0.06) |
| 7.5  (CSP4) | 8.22(0.15) | 1.28(0.14) | 0.10(0.10) |
| 18.2 (CSP6) | 8.93(0.03) | 0.64(0.02) | 0.13(0.01) |
| 23.8 (CSP9) | 8.71(0.42) | 0.00(0.00) | 0.16(0.02) |

**Table S10**. The relative percentage population, pop. %, of Ce clusters containing $m$ Ce atoms.

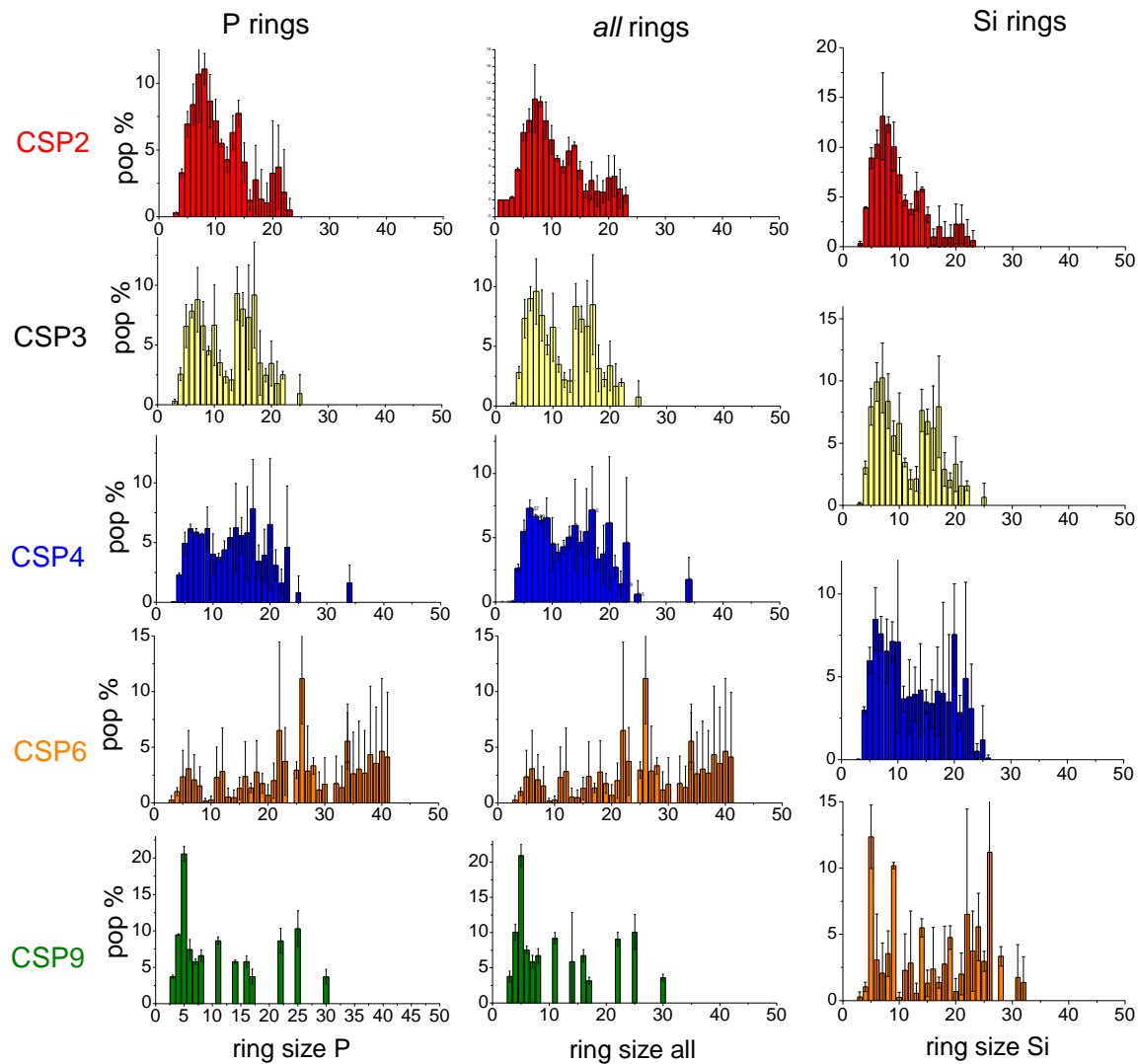| $M$ | Pop % | | | | |
|---|---|---|---|---|---|
| | CSP2 | CSP3 | CSP4 | CSP6 | CSP9 |
| 1 | 95.5 | 92.8 | 84.8 | 60.4 | 60.8 |
| 2 | 4.5 | 5.8 | 7.6 | 18.9 | 20.1 |
| 3 | 0.0 | 1.4 | 4.8 | 11.0 | 8.4 |
| 4 | 0.0 | 0.0 | 2.8 | 5.5 | 3.4 |
| 5 | 0.0 | 0.0 | 0.0 | 2.4 | 1.6 |
| 6 | 0.0 | 0.0 | 0.0 | 0.6 | 1.6 |
| 7 | 0.0 | 0.0 | 0.0 | 0.0 | 1.1 |
| 8 | 0.0 | 0.0 | 0.0 | 0.6 | 0.6 |
| 9 | 0.0 | 0.0 | 0.0 | 0.0 | 0.0 |
| 10 | 0.0 | 0.0 | 0.0 | 0.0 | 0.6 |
| 11 | 0.0 | 0.0 | 0.0 | 0.0 | 0.6 |
| 12 | 0.0 | 0.0 | 0.0 | 0.0 | 0.0 |
| 13 | 0.0 | 0.0 | 0.0 | 0.0 | 0.6 |
| 14 | 0.0 | 0.0 | 0.0 | 0.6 | 0.6 |
| $\bar{m}$ | 1.05 | 1.09 | 1.26 | 1.76 | 1.99 |

**Figure S1**. Ring size analysis for Si (CSP2, CSP3, CSP4, CSP6), P (all glasses) and *all* formers without distinction. Different colors mean different compositions. Si rings analysis for CSP9 was omitted because of the small amount of $SiO_2$ in the glass.
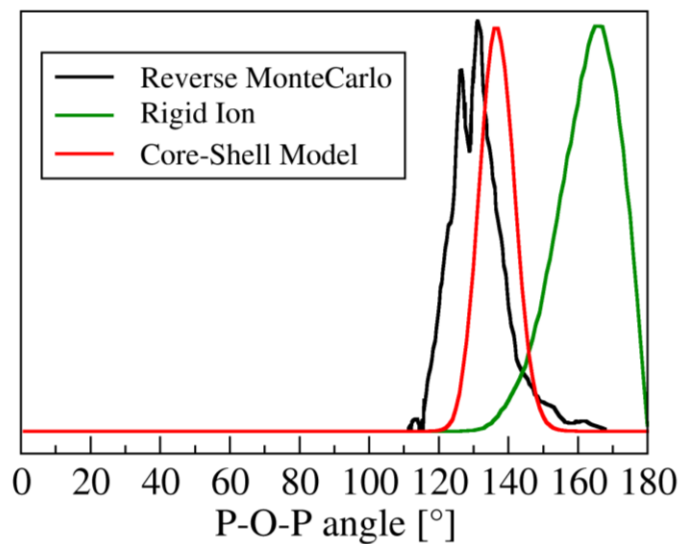
**Figure S2**. The P-O-P intertetrahedral angle distributions of the CaO-$P_2O_5$ glass obtained with a Reverse Monte Carlo approach on diffraction data[4] is compared to those provided by the RI model (green curves) and the CS model (red curves).

**Bibliography**

(1) Rygel, J. L. Cerium clustering and radiation damage resistance in aluminophosphate and silicophosphate glasses. PhD. Thesis . The Pennsylvania State University.

(2) Pickup, D. M.; Ahmed, I.; Guerry, P.; Knowles, J. C.; Smith, M. E.; Newport, R. J. The structure of phosphate glass biomaterials from neutron diffraction and 31P nuclear magnetic resonance data. *J. Phys.: Condens. Mat.* **2007,** *19* (14), 415116-415116.

(3) Du, J.; Kokou, L.; Rygel, J. L.; Chen, Y.; Pantano, C. G.; Woodman, R.; Belcher, J. Structure of Ce phosphate glasses: molecular dynamics simulation. *J. Am. Cer. Soc.* **2011,** *94* (8), 2393-2401.

(4) Wetherall, K. M.; Pickup, D. M.; Newport, R. J.; Mountjoy, G. The structure of calcium metaphosphate glass obtained from x-ray and neutron diffraction and reverse Monte Carlo modelling. *J. Phys.: Condens. Mat.* **2009,** *21* (3), 035109.